

Triangularity effects on the collisional diffusion for elliptic tokamak

P. Martín, and E. Castro

*Departamento de Física, Universidad Simón Bolívar, Apdo. 89000,
Caracas 1080A, Venezuela.*

Abstract

The effect of ellipticity and triangularity will be analyzed for axisymmetric tokamak in the collisional regime. Analytic forms for the magnetic field cross sections are taken from those derived recently by other authors. Analytic results can be obtained in elliptic plasmas with triangularity by using a special system of tokamak coordinates recently published. Our results show that triangularities smaller than 0.6 increases confinement for ellipticities in the range 1.2 to 2. This behavior happens for negative and positive triangularities, however this effect is stronger for negative than for positive triangularities. The maximum diffusion velocity is not obtained for zero triangularity, but for small negative triangularities. Ellipticity is also very important in confinement, but the effect of triangularity seems to be more important. High electric inductive fields increases confinement, though this field is difficult to modify once the tokamak has been built. The analytic form of the current produced by this field is like that of a weak Ware pinch with an additional factor, which weakens the effect by an order of magnitude. The dependence of the triangularity effect with the Shafranov shift is also analyzed.

Key words: Triangularity, collisional diffusion, current holes, tokamaks

PACS: 52.55.Dy, 52.55.Fa

1. Introduction

The tokamak (toroidal magnetic camera) seem to be the most promising alternative for the future fusion reactors on controlled nuclear fusion [1]. The nuclear fusion of the nuclei of deuterium and tritium to produce α particles (nuclei of helium), neutrons and energy, has the advantage over the nuclear fission, that there is not heavy radioisotopes of large half-life. High temperature is required in order to produce this nuclear reactions in a large scale, which in the hydrogen bomb is obtained with a nuclear fission bomb. It is also required adequate densities and confinement time for the fuel particles in the thermonuclear fusion. The first tokamaks were toroides of circular cross sections, but the future generation of tokamaks (i.e. ITER) are like ellipses with triangularity and other types of deformation.

Most of the theories on confinement and instabilities were developed for circular cross sections at the beginning, but later the analysis were extended to more general configurations, mainly through computer simulations. However, new development in tokamaks coordinates seems[2-6] ap-

propriated to treat this general plasma shapes in a theoretical way, obtaining most general conclusions than those got by computed simulations, where each change of parameter requires a complete new simulation. In this work plasma tokamak confinement is study for a general kind of plasma configurations including ellipticity and triangularity, as well as nonlinear flows, in the low vorticity approximation This new treatment does not include anomalous diffusion and turbulence, that is, it seems suitable for the H-mode, where the existence of internal barriers and shear produce a large scale decreasing in turbulence. Our analysis however has been extended also to plasma configuration with current holes, since recently has been found that this particularity appears in most of the large tokamaks in operation. As consequence this topic has become very important, and the new analysis, here performed, shows an improvement in confinement due to current holes.

In some way the present paper extends our previous and recent analysis on confinement [6], including now non-linear terms or flows and current holes. Our previous work on conserved quantities and extended Grad-Shafranov equation for plasmas with non-linear flows [5] is used now as an starting point for the diffusion problem.

It is interesting to point out that whilst vorticity, could

Email addresses: pmartin@usb.ve (P. Martín,), ecastro@usb.ve (E. Castro).

be important within an internal barrier, however outside the barrier, turbulence is low, and therefore vorticity, which is associated with turbulence, will be also low, then in some way can be neglected.

Axisymmetric tokamaks will be considered here. In Section II and III theoretical treatment and results will be describe, respectively, and the last Section (Sec. 4) will be devoted to discussion and conclusion.

2. Theoretical treatment

The starting point is the steady state MHD equation [Eq.(1) in Ref.[5]]

$$\rho \vec{v} \cdot \nabla \vec{v} = \frac{1}{c} \vec{j} \times \vec{B} - \nabla p . \quad (1)$$

From here it is obtained

$$\rho \nabla F = \frac{1}{c} \vec{j} \times \vec{B} + \vec{v} \times \vec{\omega} , \quad (2)$$

where the auxiliary function F were already defined as [5]

$$F(\vec{v}, \rho, T) = \frac{v^2}{2} + W(\rho, T) , \quad (3)$$

being $W(\rho, T)$ the enthalpy given as [5,7]

$$W(p, T) = \int^p \frac{1}{\rho} \frac{\partial p}{\partial \rho} d\rho . \quad (4)$$

This integral is performed along a magnetic line, where T can be considered constant, since as is well known, the heat transference along a magnetic lines is very fast. Now if the vorticity is neglected then Eq.(2) becomes

$$\rho \nabla F = \frac{1}{c} \vec{j} \times \vec{B} , \quad (5)$$

and from here

$$\vec{B} \cdot \nabla F = 0 , \quad (6)$$

in this way F becomes constant on a magnetic surface. Eq.(8) is similar to Eq. (4.2.2) in Ref. [1], once the pressure p is changed for our new function F , previously defined. Diffusion including triangularity and ellipticity on the collisional regime without non-linear terms has been also treated for us recently [6], and some of the first results will look with some similarity to those previous ones [7].

The important function $\mu(\tilde{\sigma}, \tilde{s})$ appears also in this work as in the previous ones

$$\mu(\tilde{\sigma}, \tilde{s}) = \exp \left[- \int_0^s \kappa_\sigma ds \right] = \frac{1}{h_\sigma(\tilde{\sigma}, \tilde{s})} , \quad (7)$$

where κ_σ is the point curvature of the family of curves orthogonal to magnetic lines, and h_σ is one of the scale factors for the new orthogonal curvilinear coordinates $\tilde{\sigma}$ and \tilde{s} .

To study diffusion in the scrape off layer (SOL) surface the normal velocity will be

$$\bar{v} = \left(\oint R ds \right)^{-1} \oint \left(-\eta_\perp \frac{\partial F}{\partial \sigma} - E_p B_\varphi + E_\varphi B_p \right) B^{-2} R ds. \quad (8)$$

By using the continuity equation

$$\nabla \cdot \vec{j} = 0 , \quad (9)$$

as well as the univaluation for the electric potential $\phi(\vec{r}, t)$, the value of the parallel velocity can be obtained as

$$j_{\parallel} = - \frac{\rho B_\varphi}{c B B_p} \frac{\partial F}{\partial \sigma} + G(\tilde{\sigma}) B , \quad (10)$$

where

$$G(\tilde{\sigma}) = \left[\oint \frac{\rho B_\varphi}{B_p^2} \frac{\partial F}{\partial \sigma} ds + \frac{1}{\eta_{\parallel}} \oint \frac{E_\varphi B_\varphi}{B_p} ds \right] / \left(\oint \frac{B^2}{B_p} ds \right). \quad (11)$$

Here the density around a magnetic surface is difficult to determine, however for some simplified cases [8], $\rho(\psi)$ is given by

$$\rho(\psi) = \rho_0(\psi) \exp(\omega^2 \gamma^2 / 2T) , \quad (12)$$

where ψ is the poloidal magnetic flux. If ω is neglected as we did at the beginning, then ρ will be constant on a magnetic surface.

In any case ρ could be also treated as an average value $\bar{\rho}$ for each magnetic surface, that is

$$G(\tilde{\sigma}) = [\bar{\rho} \oint \frac{B_\varphi}{B_p^2} \frac{\partial F}{\partial \sigma} ds + \frac{1}{\eta_{\parallel}} \oint \frac{E_\varphi B_\varphi}{B_p} ds] / \left(\oint \frac{B^2}{B_p} ds \right). \quad (13)$$

Furthermore, the condition that $\nabla \times (\nabla F) = 0$, leads to the equation

$$\frac{\partial F}{\partial \sigma} = \left(\frac{\partial F}{\partial \sigma} \right)_1 \mu(\tilde{\sigma}, \tilde{s}) , \quad (14)$$

where $\mu(\tilde{\sigma}, \tilde{s})$ was previously defined and the subindex 1 is used to denote the outermost point of the magnetic surface.

Finally using all our previous approximations the average normal velocity \bar{v} will be

$$\bar{v} = - \frac{\bar{\rho} \eta_\perp}{B_{\varphi_1}^2} \left(\frac{\partial F}{\partial \sigma} \right)_1 \frac{1}{\tilde{I}_0} \left[\frac{\tilde{I}_1}{\tilde{R}_1^2} + \frac{\eta_{\parallel}}{\eta_\perp \tilde{\gamma}_1 \tilde{R}_1} \left(\tilde{I}_3 - \frac{\tilde{I}_1^2}{\tilde{I}_4} \right) \right] - \frac{E_{\varphi_1}}{B_{\varphi_1} \tilde{\gamma}_1 \tilde{I}_0} \left[\tilde{I}_7 - \frac{\tilde{I}_1 \tilde{I}_6}{\tilde{I}_4} + \tilde{\gamma}_1^2 \tilde{I}_5 \right] \quad (15)$$

where R_m is the major radius of minor axis and

$$\gamma_1 = \frac{B_{p_1}}{B_{\varphi_1}} , \quad \tilde{R} = \frac{R}{R_m} , \quad d\tilde{s} = \frac{ds}{R_m} , \quad (16)$$

All the previous integrals are written in a dimensionless way as

$$\tilde{I}_0 = \oint \tilde{R} d\tilde{s} , \quad (17)$$

$$\tilde{I}_1 = \oint \tilde{R} \tilde{\mu}(s)^{-1} d\hat{s} , \quad (18)$$

$$\tilde{I}_2 = \oint \tilde{R}^3 \tilde{\mu}(s) (1 + \tilde{\gamma}_1^2 \tilde{\mu}(s)^2)^{-1} d\hat{s} , \quad (19)$$

$$\tilde{I}_3 = \oint \tilde{R}^3 (1 + \tilde{\gamma}_1^2 \tilde{\mu}(s)^2)^{-1} \tilde{\mu}(s)^{-1} d\hat{s} , \quad (20)$$

$$\tilde{I}_4 = \oint (1 + \tilde{\gamma}_1^2 \tilde{\mu}(s)^2) \tilde{\mu}(s)^{-1} \tilde{R}^{-1} d\hat{s} , \quad (21)$$

$$\tilde{I}_5 = \oint (1 + \tilde{\gamma}_1^2 \tilde{\mu}(s)^2)^{-1} \tilde{\mu}(s) \tilde{R} d\hat{s} , \quad (22)$$

$$\tilde{I}_6 = \oint \tilde{\mu}(s)^{-1} \tilde{R}^{-1} d\hat{s} , \quad (23)$$

$$\tilde{I}_7 = \oint (1 + \tilde{\gamma}_1^2 \tilde{\mu}(s)^2)^{-1} \tilde{\mu}(s)^{-1} \tilde{R} d\hat{s} . \quad (24)$$

3. Results

As in previous work in order to perform the diffusion calculation including non-linear flows, the family of selected magnetic surfaces will be identify by the equation

$$\tilde{R}(\lambda, \theta) = \frac{R(\lambda, \theta)}{R_m} = 1 + \tilde{a} \lambda \cos\theta - \lambda^2 \left(\tilde{\Delta} + \frac{\tilde{a} T(a)}{4} (1 - \cos 2\theta) \right) , \quad (25)$$

$$\tilde{z}(\lambda, \theta) = \frac{z(\lambda, \theta)}{R_m} = \tilde{a} \lambda E(a) \sin\theta - \frac{\lambda^2 \tilde{a} E(a) T(a)}{4} \sin 2\theta , \quad (26)$$

where λ is the parameter identifying each magnetic surface and. Here all the quantities and variables with tilde are dimensionless, that is

$$\tilde{a} = \frac{a}{R_m} , \quad \tilde{\Delta} = \frac{\Delta(a)}{R_m} . \quad (27)$$

$E(a)$ and $T(a)$ are elliptic and triangularity distortion, respectively.

As in previous work [6] it is more convenient to define also dimensionless velocity as

$$\tilde{v} = \frac{\bar{v}}{\bar{v}_{oc}} , \quad (28)$$

where \bar{v}_{oc} is the normal velocity when ellipticity and triangularity are zero, that is,

$$\bar{v}_{oc} = -\frac{\eta_{\perp} \bar{\rho}}{B_{\varphi_1}^2} \left(\frac{\partial F}{\partial \sigma} \right)_1 \alpha_0 , \quad (29)$$

and α_0 is defined by

$$\alpha_0 = \frac{\hat{I}_2(0)}{\hat{R}_1^2} + \frac{\eta_{\parallel}}{\eta_{\perp}} \frac{1}{\hat{R}_1^2 \tilde{\gamma}_1^2} \left(\hat{I}_3(0) - \frac{\hat{I}_1(0)^2}{\hat{I}_4(0)} \right) , \quad (30)$$

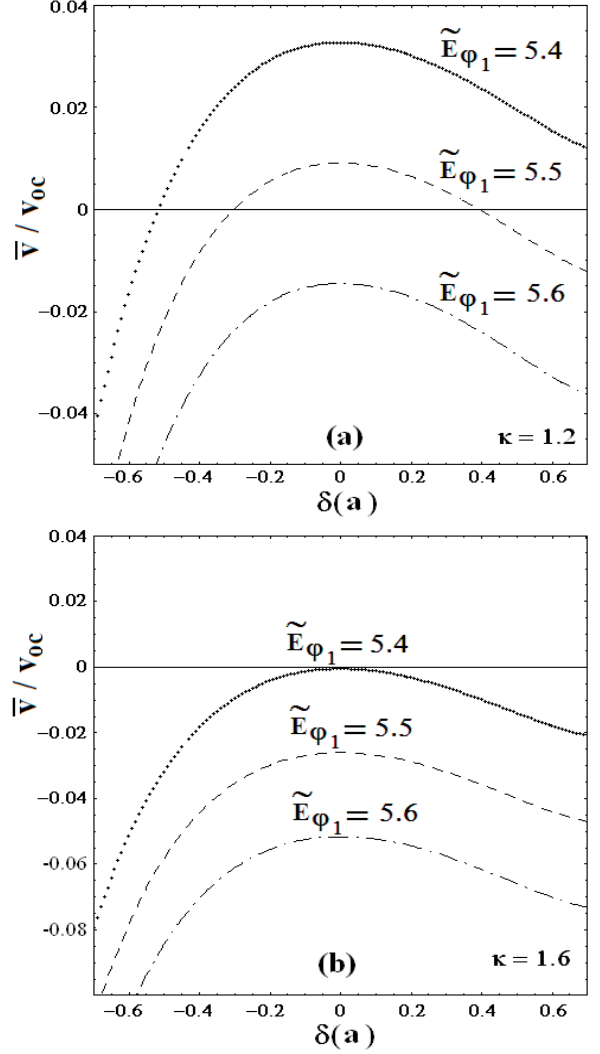


Fig. 1. Dimensionless diffusion velocity versus triangularity for three different dimensionless inductive fields $\tilde{E}_{\varphi_1} = 5.4$ (point line), 5.5 (dash line) and 5.6 (dash-point line). Fig.(1a) and (1b) are respectively for elongations $\kappa(a) = 1.2$ and 1.6

Dimensionless inductive electric field is also used defined by

$$\tilde{E}_{\varphi_1} = \frac{E_{\varphi_1}}{-\frac{\eta_{\perp} \bar{\rho}}{B_{\varphi_1}} \left(\frac{\partial F}{\partial \sigma} \right)_1} . \quad (31)$$

In figure 1, the dimensionless velocities are show as a function of the triangularity for three different values of dimensionless electric field and for a given elliptic elongation, which are 1.2 and 1.6, in Figure 1a and 1b, respectively.

These results show that positive and negative triangularities increases confinement. Since confinement corresponds to negative values of diffusion velocity. The points where the velocities are zero, correspond to marginal confinement, that is, to zero diffusion velocity. The worst situation is just at the maximum of the curves, which is usually near $\delta(a) \cong 0$, thought not always exactly for zero triangularity. There are in general better confinement with negative triangularity than with positive ones, since for the same absolute value of triangularities the absolute value of the

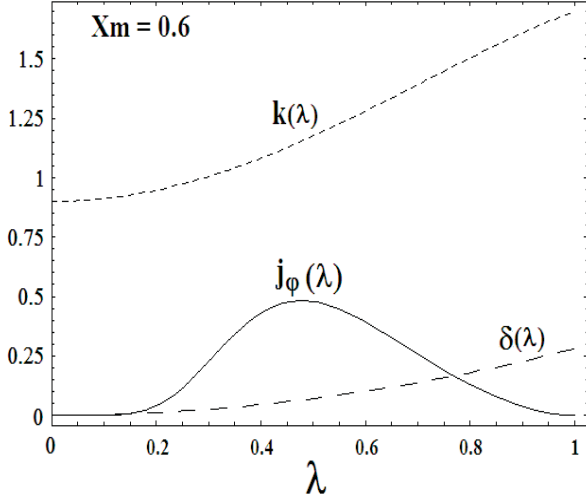


Fig. 2. Current density profile, elongation and triangularity along the major radius. The parameter λ identifies each magnetic surface and the value of the parameter x_m is shown on upper-left corner

negative velocities are larger in the negative side of $\delta(a)$. Furthermore the triangularity tends to a plateau for positive large values of $\delta(a)$, and that plateau does not appear in the negative side of $\delta(a)$, at least for the range of parameters here investigated.

Ellipticity is also important in confinement, as can be see looking the Figures (1a) and (1b). There are better confinement for elliptic elongation $k(a) = 1.6$ than for $k(a) = 1.2$. However, in this work the analysis is carried out mainly on triangularity effects.

Here, we are also interested on find out the differences on diffusion due to current holes. In this case the Shafranov shift, triangularity and elliptic elongation are taken from the work of V. Yavorsky et al. [9]. They definitions are

$$\Delta(\lambda) = \Delta_0 (1 - \lambda^2) \quad . \quad (32)$$

$$\Lambda(\lambda) = \Lambda_a \lambda^2 \quad . \quad (33)$$

$$k(\lambda) = k_a - (k_a - k_0) (1 - \lambda^2)^2 - 0.5 k'_a \lambda^2 (1 - \lambda^2) \quad . \quad (34)$$

where Λ_a denote the triangularity, instead of the usual notation $\delta(\lambda)$. The parameter λ denoting as usual the magnetic surface, which is also defined as

$$\lambda = \frac{\tilde{\sigma}}{a} = \frac{r}{a} \quad . \quad (35)$$

In the above paper, a parameter x_m is introduce in order to adjust the analytic form to the experimental data. The calculation here will be carried out for the Japanese tokamak JT-60U, and for this device a good value of x_m is 0.6. This parameter determine another parameter m by

$$m = \frac{3((1 - x_m)^{-6} - 1)}{(1 + x_m^{-1})} \quad , \quad (36)$$

used in the analytic form for j_φ

$$j_\varphi = (1 - \lambda^2)^2 (1 - (1 - \lambda)^6)^{2m} \quad , \quad (37)$$

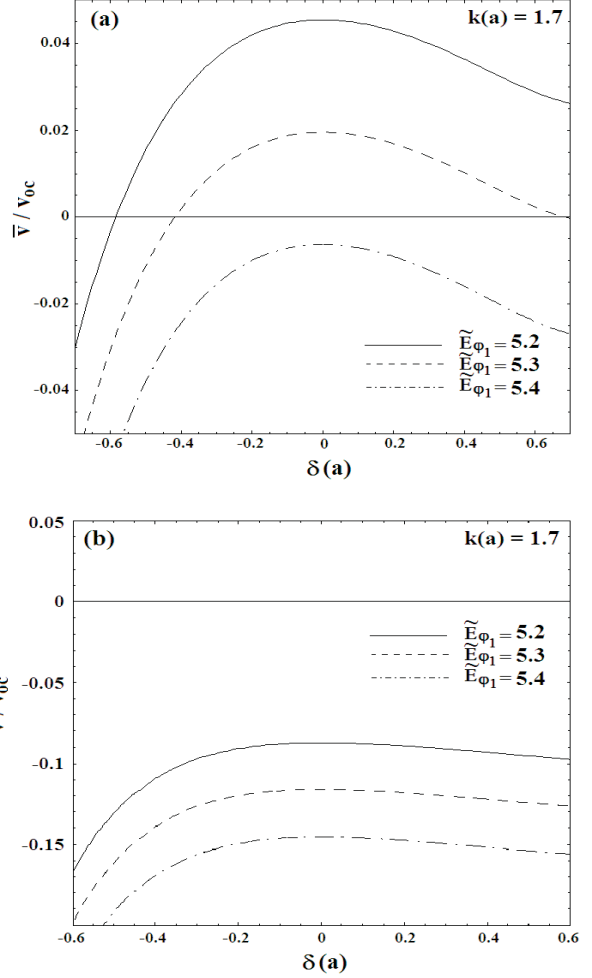


Fig. 3. Dimensionless diffusion velocity versus triangularity for elongation $k(a) = 1.7$, in the scrape-off layer surface, and three different dimensionless inductive fields $\tilde{E}_{\varphi_1} = 5.2$ (plain line), 5.3 (dash line) and 5.4 (dash-point line). Figure (3a) is for plain currents with no-holes, and Fig. (3b), when current holes are present.

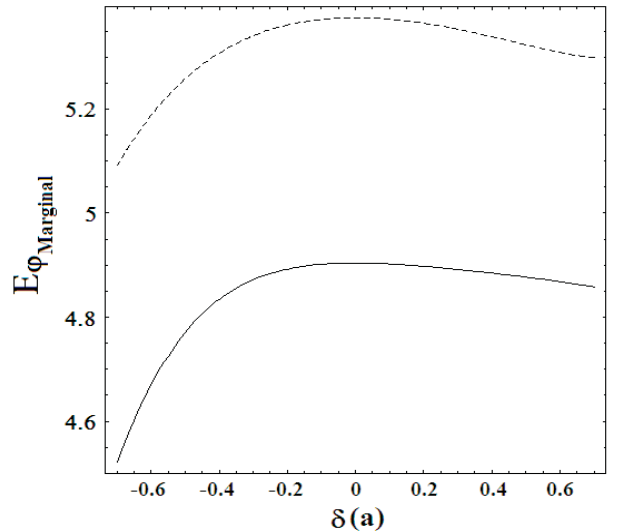


Fig. 4. Marginal dimensionless inductive field as a function of triangularity for plasma configurations with current holes (plain line) and without current holes (dash line)

this equation is well adjusted to the experimental values. Fig. 2 shows this current along the cross section. The minor magnetic axis is as usually as $\lambda = 0$, and the current hole is about 1/10 of the plasma size measured by a . All the previous definitions allow to determine κ_σ , and from here our μ parameter, which is used elongation $k(a) = 1.7$ without and with current hole, later to determine the dimensionless normal velocity \tilde{v} .

The results are given in Fig.(3a) and (3b). Looking the results, there is a clear improvement in confinement. The patterns however are a little different, since when the current holes are present the plateau for large positive triangularities are more ample than in the case with no hole. The comparison between the results without or with current holes is better carried out using the marginal inductive field, that is, the values where the normal velocity are zero. These curves separate the confinement region from the no-confinement region, characterized by negative or inward diffusion velocities.

Figure 4, shows $E_{\varphi marginal}$ as a function of triangularity for elliptic elongation $k(a) = 1.7$. The improvement in confinement due to the hole current is actually very important. In the worst situation for this elongation, the velocity is about 20 and 25% larger when the current hole is present.

4. Conclusion and Discussion

Non-linear collisional transport in axisymmetric tokamaks has been analyzed including non-linear flows for toroidal plasma configurations with ellipticity and triangularity in the low vorticity limit. This generalizes previous linear treatments recently published [6]. The normal velocity in the scrape-off layer surface has been determine for a general plasma configuration. The results are given as a function of several integrals around some magnetic curves. Numerical calculations has been carried out using equations for the magnetic surfaces consistent with Grad-Shafranov equations, which are nonlinear in the parameter λ , characterizing each magnetic surface.

Numerical calculations on diffusion velocities have been also carried out for plasma configuration with current holes, characteristic in the experiments with large tokamaks. The present analysis is mainly concentrated in the effects on diffusion due to different triangularities .

Collisional confinement improves when triangularity is present in the tokamak plasma configuration. However, the effect of negative triangularity is more significative than positive ones. In the range of parameters here analyzed (-0.6 to 0.6) appears a plateau tendency in the diffusion velocity for positive triangularities, but not for negative ones. Ellipticity is also important in confinement but a complete analysis of this theme will be carried out in future works.

The influence on confinement due to current holes in the plasma is also analyzed here. The present results show an slight improvement in confinement when current holes are present. In this case the pattern of the curves look in some

way similar to the case where there is not hole, but the plateaus formation for positive triangularities is clearer and with larger extension. This effect is complementary to the confinement increasing.

Though the numerical calculations are carried out for some selected tokamaks, however our treatment is very general, and not limited to these cases. In our analysis dimensionless variables are used most of the time in order of reach more general results, and it seems that the present work should be useful in future tokamaks designs.

5. Acknowledgements

The present work was supported by the Decanato de Investigaciones (Research Dean) of the Universidad Simón Bolívar (GID-22).

References

- [1] Wesson J. Tokamaks. The Oxford Engineering Science Series;48, Oxford University Press, Inc..New York (Second Edition); 1997. Chapters 1 and 2, and p. 147.
- [2] Martín P. Magnetohydrodynamics treatment of collisional transport in toroidal configurations: Application to elliptic cross sections. Phys. Plasmas 2000; 7(7): 2915-2922.
- [3] Martín P and Haines M G. Poloidal magnetic field around a tokamak magnetic surface. Phys. Plasmas 1998; 5(2): 410-416.
- [4] Martín P, Haines M G and Castro E. Current density and poloidal magnetic field for toroidal elliptic plasmas with triangularity. Phys. Plasmas 2005; 12(8): 082506 (1-15)
- [5] Martín P, Castro E and Haines M G. Conserved functions and extended Grad-Shafranov equation for low vorticity viscous plasmas with nonlinear flows. Phys. Plasmas 2005; 12(10): 102505 (1-7)
- [6] Martín P, Castro E and Haines M G. Collisional diffusion in toroidal plasmas with elongation and triangularity. Phys. Plasmas 2007; 14(Issue 4 or 5);1-10 (in press)
- [7] Guazzotto L, Betti R, Manickam J and Kaye S. Numerical study of tokamak equilibria with arbitrary flow. Phys. Plasmas 2004; 11(2): 604-614.
- [8] Il'gisonis V I and Pozdnyakov Yu I. Suppression of the Magnetic Surface Shift by Plasma Rotation in a Tokamak. JETP Letters 2000; 71(8): 314-317
- [9] Yavorskij V, Coloborod'ko V,Schoepf K, Sharapov S E, Challis C D, Resnik S and Stork D, Confinement of fusion alpha-particles in JET hollow current equilibrium. Nucl. Fusion 2003; 43(10): 1077-1090.